PO Box 2345, Beijing 100023, China
www.wjgnet.com
wjg@wjgnet.com

ELSEVIER

World J Gastroenterol 2005;11(47):7418-7429
World Journal of Gastroenterology ISSN 1007-9327

• *BASIC RESEARCH* •

Hepatocyte cytoskeleton during ischemia and reperfusion - influence of ANP-mediated p38 MAPK activation

Melanie Keller, Alexander L Gerbes, Stefanie Kulhanek-Heinze, Tobias Gerwig, Uwe Grützner, Nico van Rooijen, Angelika M Vollmar, Alexandra K Kiemer

Melanie Keller, Stefanie Kulhanek-Heinze, Tobias Gerwig, Angelika M Vollmar, Alexandra K Kiemer, Department of Pharmacy, Centre of Drug Research, University of Munich, Butenandtstr. 5-13, 81377 Munich, Germany
Alexander L Gerbes, Tobias Gerwig, Alexandra K Kiemer, Department of Medicine II, Klinikum Großhadern, University of Munich, Marchionistr. 17, 81377 Munich, Germany
Uwe Grützner, Institute for Surgical Research, Klinikum Großhadern, University of Munich, Marchionistr. 17, 81377 Munich, Germany
Nico van Rooijen, Vrije Universiteit, VUMC, Department of Molecular Cell Biology, Faculty of Medicine, 1081 BT Amsterdam, The Netherlands
Supported by the Deutsche Forschungsgemeinschaft, DFG-FOR 440/1. M.K. was supported by the LMU Munich, grant GVBI. S.527
Correspondence to: Alexandra K Kiemer, PhD, Professor of Pharmaceutical Biology, Saarland University, P.O. Box 15 11 50, D-66041 Saarbrücken,
Germany. pharm.bio.kiemer@mx.uni-saarland.de
Telephone: +49-681-302-57301 Fax: +49-681-302-57302
Received: 2005-01-31 Accepted: 2005-04-18

Abstract

AIM: To determine functional consequences of this activation, whereby we focused on a potential regulation of the hepatocyte cytoskeleton during ischemia and reperfusion.

METHODS: For *in vivo* experiments, animals received ANP (5 μg/kg) intravenously. In a different experimental setting, isolated rat livers were perfused with KH-buffer ±ANP (200 nmol/L)±SB203580 (2 μmol/L). Livers were then kept under ischemic conditions for 24 h, and either transplanted or reperfused. Actin, Hsp27, and phosphorylated Hsp27 were determined by Western blotting, p38 MAPK activity by *in vitro* phosphorylation assay. F-actin distribution was determined by confocal microscopy.

RESULTS: We first confirmed that ANP preconditioning leads to an activation of p38 MAPK and observed alterations of the cytoskeleton in hepatocytes of ANP-preconditioned organs. ANP induced an increase of hepatic F-actin after ischemia, which could be prevented by the p38 MAPK inhibitor SB203580 but had no effect on bile flow. After ischemia untreated livers showed a translocation of Hsp27 towards the cytoskeleton and an increase in total Hsp27, whereas ANP preconditioning prohibited translocation but caused an augmentation of Hsp27 phosphorylation. This effect is also mediated via p38 MAPK, since it was abrogated by the p38 MAPK inhibitor SB203580.

CONCLUSION: This study reveals that ANP-mediated p38 MAPK activation leads to changes in hepatocyte cytoskeleton involving an elevation of phosphorylated Hsp27 and thereby for the first time shows functional consequences of ANP-induced hepatic p38 MAPK activation.

Key words: Hormonal preconditioning; Atrial natriuretic peptide; Hsp 27; Actin; Polymerization

Keller M, Gerbes AL, Kulhanek-Heinze S, Gerwig T, Grützner U, van Rooijen N, Vollmar AM, Kiemer AK. Hepatocyte cytoskeleton during ischemia and reperfusion – influence of ANP-mediated p38 MAPK activation. *World J Gastroenterol* 2005; 11(47): 7418-7429
http://www.wjgnet.com/1007-9327/11/7418.asp

INTRODUCTION

Ischemia/reperfusion injury (IRI) remains a serious problem after liver surgery or liver transplantation, as it is a major cause of primary nonfunction or dysfunction of the graft[1-3]. In previous studies, we could demonstrate that atrial natriuretic peptide (ANP) has protective effects on the liver *ex vivo,* as reperfusion damage in ANP-preconditioned organs after cold and warm ischemia was significantly reduced[4-6]. Recently, Cottart *et al*[7]. also demonstrated beneficial properties of the peptide on the liver after ischemia *in vivo*. We have previously shown that preconditioning with ANP increases p38 mitogen activated kinase (MAPK) activity in the liver[8]. Enhanced p38 MAPK activity was reported to contribute to the protection against hepatic IRI in models of ischemic preconditioning (IPC)[9,10]. Furthermore, other groups assigned an important role to p38 MAPK in protection against IRI in the heart[11,12].

In contrast, ANP's cytoprotective effects in post-ischemic livers are independent of an activation of the p38 MAPK but are mediated via an activation of protein kinase A[13]. Accordingly, the functional significance of an ANP-

mediated p38 MAPK activation in the liver after ischemia/reperfusion (I/R) remains unknown. We therefore studied a potential functional role of p38 MAPK in the regulation of the hepatocyte cytoskeleton following I/R.

Structural alterations of the cytoskeleton, such as changes of cell shape of hepatocytes, sinusoidal endothelial cells (SEC), and platelets have been reported to cause disturbances of intracellular transport processes, cell motility, and microcirculation following I/R leading to dysfunction of the organ (for review see Refs.[14-16]). The subcellular distribution of filamentous actin (F-actin), being an important component of the cytoskeleton, as well as the balance between F-actin and monomeric G-actin seem to largely determine the functional outcome[17-19]. In liver cells F-actin forms microfilaments, which are involved in intracellular transport processes, exo- and endocytosis, maintenance of cell shape, and canalicular motility responsible for bile flow[14,18,19]. They are located particularly around the bile canaliculi exhibiting regulatory functions on bile secretion[17,20], but also in the apical membrane region of hepatocytes ensuring stability and mobility[21]. In hepatocytes, a decrease in hepatic F-actin content determines inhibition of store-operated calcium-channels (SOCs), disruption of the organization of the endoplasmic reticulum, and functional disturbances of tight junctions[19,22,23]. Cytoskeletal disruption caused by the administration of phalloidin or by chemical hypoxia results in decreased bile flow and plasma membrane breakdown in liver cells[15,24]. Shinohara *et al*[25]. proved that after warm ischemia *in vivo*, F-actin is reduced in rabbit livers resulting in the loss of cell-integrity and cytoplasmic transport in the liver causing damage to organelles and changes in cell morphology. The small heat shock protein Hsp27, which corresponds to Hsp25 in rodents and is able to interact with the cytoskeleton, plays an important role in the regulation of actin dynamics in other cell types[26-30]: Its phosphorylation leads to an increased conversion of monomeric G-actin into actin filaments (F-actin)[31], while unphosphorylated Hsp27 inhibits the polymerization of actin by binding to the capping end of actin filaments[32,33]. Its functions have been thoroughly investigated in the heart, suggesting an involvement of the heat shock protein in cardioprotection after IPC *in vitro* and *in vivo*[12,34].

The phosphorylation of Hsp27 is exhibited by the p38 MAPK/MAPKAPK2 pathway in different cells and organ systems, but has as yet been unknown in the liver[35-38]. As mentioned above, ANP activates the p38 MAPK in the liver. Due to the lack of knowledge about the downstream targets and functional consequences of this hepatic p38 MAPK activation by ANP, we aimed to determine a potential link to cytoskeletal alterations during I/R. Since the reported activation of p38 MAPK by ANP was detected as an early signaling event after preconditioning[8], we focused on early pre- and post-ischemic events.

MATERIALS AND METHODS

Materials

Rat ANP and SB203580-HCl were purchased from Calbiochem/Novabiochem (Bad Soden, Germany). Complete® was from Roche Diagnostics GmbH (Mannheim, Germany), recombinant murine Hsp25 and rabbit anti-Hsp25 polyclonal antibody from StressGen Biotechnologies (Victoria, Canada), rabbit anti-phospho-Hsp27 polyclonal antibody from New England Biolabs GmbH (Frankfurt, Germany), mouse anti-actin monoclonal antibody from Chemicon International (Hofheim, Germany), rabbit anti-p38 polyclonal antibody from Calbiochem-Novabiochem (Bad Soden, Germany), peroxidase conjugated goat anti-rabbit-IgG antibody from Dianova (Hamburg, Germany), and goat anti-mouse-IgG1 antibody conjugated to horseradish peroxidase from BIOZOL (Eching, Germany).

All other materials were purchased from either Sigma (Deisenhofen, Germany), or VWR international™ (Munich, Germany).

Animals

Male Sprague-Dawley rats weighing 200-300 g or male Lewis rats (donors: 207±12 g; recipients: 276±18 g body mass) were purchased from Charles River Wiga GmbH (Sulzfeld, Germany) and housed in a climatized room with a 12-h light-dark cycle. The animals had free access to chow (Sniff, Soest, Germany) and water up to the time of experiments. All animals received humane care according to the guidelines for care and use of laboratory animals. The study was registered with the local animal welfare committee.

ANP treatment

Under anesthesia Lewis rats received an intravenous infusion of ANP (5 μg/kg) or NaCl for 20 min. Thereafter, livers were excised, kept in cold UW solution (4 °C) for 24 h, transplanted into the recipient animal and reperfused for up to 2 h. At the indicated times (after 20-min perfusion, 24-h ischemia, 2-h reperfusion), livers were frozen in liquid nitrogen. Bile was collected during perfusion and reperfusion and quantified volumetrically. The bile flow was calculated per minute and gram liver tissue.

For isolated perfused rat liver experiments, Sprague-Dawley rats were anesthetized with Narcoren® (Merial, Hallbergmoos, Germany, 50 mg/kg body weight, intraperitoneally), 250 IU heparin were administered, the portal vein was cannulated, and the liver was perfused *in situ* with hemoglobin-free and albumin-free bicarbonate buffered Krebs-Henseleit (KH) solution (pH 7.4, 37 °C) gassed with 95% O_2 and 50 mL/L CO_2. The perfusion medium was pumped through the liver with a membrane pump at a constant flow rate in a non-recirculating fashion[5]. After 10 min of perfusion, ANP (200 nmol/L) was added to the perfusion buffer (depending on the treatment group), followed by an additional perfusion for 20 min. In some groups, SB203580 was added to the perfusion buffer from the beginning of perfusion followed by 30 min of perfusion. After these pretreatment procedures, livers were perfused with 30 mL of cold (4 °C) University of Wisconsin (UW) solution (DuPont Pharma

GmbH, Bad Homburg, Germany) for 1 min and stored in UW solution (4 °C) for 24 h. After this period of ischemia, the liver was reperfused with KH solution for up to 45 min. At the indicated times (after 30-min perfusion, 24 h ischemia, 45-min reperfusion), livers were frozen in liquid nitrogen.

Homogenization and fractionation of liver tissue for Western blot analysis

A fractionation protocol was employed according to published methods with minor modifications[39,40]. Briefly, 50 mg of liver tissue were homogenized in 1.5 mL of lysis buffer (50 mmol/L Tris-HCl pH 7.0, 5 mmol/L EGTA, 1 mmol/L PMSF, 1 mmol/L sodium vanadate, 40 μL Complete®) containing 1% Triton® X-100 (Roth, Karlsruhe, Germany) with a dounce homogenizer. Centrifugation at 15 000×*g* (15 min, 4 °C) delivered the cytoskeletal fraction in the pellet; supernatants representing the cytosolic fraction were cleared by ultracentrifugation (100 000×*g*, 2.5 h, 4 °C). The pellet was resuspended in SDS-containing sample buffer and the cytosolic fraction was diluted with the same sample buffer. Samples were stored at -20 °C until use for Western blot analysis.

Immunoprecipitation

Liver tissue was homogenized as described above, but not fractionated. Protein concentration was determined by the bicinchoninic acid assay method[41]. Five hundred micrograms of protein in 500 μL lysis buffer was incubated with 5 μL of primary antibody (rabbit anti-Hsp25) with shaking overnight at 4 °C. The antibody-antigen complex was precipitated by incubation with 50 μL of washed agarose-A-beads (Sigma, Deisenhofen, Germany) for 2 h, followed by centrifugation. The beads were washed thrice with cold lysis buffer and resuspended in 25 μL of 3× SDS-containing sample buffer. After addition of 25 μL 1× sample buffer, samples were boiled for 5 min at 95 °C followed by centrifugation to remove the beads. Thirty-five microliters of the supernatant for phosphorylated Hsp27 and 10 μL for total Hsp27 were used for protein detection by Western blot analysis.

Western blot analysis

Livers were homogenized, fractionated, and treated as described above. Proteins in total liver homogenates, fractionated liver samples, or immunoprecipitates were separated by SDS-PAGE[42] and, after electrophoretical transfer, visualized via binding of specific first and HRP-conjugated secondary antibodies followed by chemoluminescent detection (NEN, Cologne, Germany). Detection and quantification was performed with a Kodak image station (NEN, Cologne, Germany).

Quantification of actin content in liver fractions

After detection of either F- or G-actin in liver samples via Western blot analysis, the densitometric intensity of the corresponding bands was used to evaluate the ratio of F-resp. G-actin referred to total actin signal (F- + G-actin) in the respective sample.

Staining of tissue sections

At the indicated times, livers were snap-frozen in liquid nitrogen and cut into 6-μm sections. Slices were dried overnight at room temperature. Before staining, samples were fixed in 3% formaldehyde for 15 min, rinsed thrice with PBS (phosphate buffered saline, pH 7.4, with calcium and magnesium), and stained with 1 U of rhodamine-conjugated phalloidin (stock solution: 200 U/mL; MoBiTec, Göttingen, Germany) and Hoechst 33342. Staining was performed for 1 h by gentle shaking in a dark room (room temperature). After two more washing steps, stained liver sections were covered with Mounting Medium (DakoCytomation GmbH, Hamburg, Germany), dried overnight, and observed by confocal laser microscopy (LSM 510 Meta, Zeiss, Jena, Germany).

Kupffer cell depletion

For Kupffer cell (KC) depletion, male Sprague-Dawley rats weighing 200-300 g were anesthetized with diethyl ether. Then 900 μL of a solution containing liposome-encapsulated Cl_2MBP were administered 48 h before perfusion experiments via a single intravenous injection into the tail vein. Animals of the control group received 900 μL NaCl instead. After injection, Cl_2MBP accumulates and induces KC apoptosis. Free Cl_2MBP released from dead macrophages has an extremely short half life in the circulation and is removed by the renal system. After 2 d, the livers of Cl_2MBP- and NaCl-pretreated rats were perfused for 30 min±ANP (200 nmol/L; 20 min), snap-frozen, and stored at -85 °C until further analysis.

Immunohistological analysis

Liver slices were fixed for 24 h in buffered formalin solution, embedded in paraffin and cut into 2 μm sections. Paraffin was removed and samples were pretreated by boiling in TRS 6 (Dako, Hamburg, Germany) in the microwave. Endogenous peroxidase was blocked by treatment with aqueous H_2O_2 solution. To verify KC depletion, ED2 as KC marker (antibody from Serotec, Oxford, England) was used. Blue staining of ED2-positive cells was realized with the ChemMate™ APAAP Kit (Dako, Hamburg, Germany) based on the alkaline phosphatase-anti-alkaline phosphatase method. The Alkaline Phosphatase Substrate Kit III (Linaris, Wertheim, Germany) served as a substrate for the alkaline phosphatase. Samples were counterstained in hematoxylin solution.

In vitro phosphorylation assay

Tissue samples (100 μg) were homogenized in ice-cold lysis buffer (containing 2 mmol/L EDTA, 137 mmol/L NaCl, 10% glycerol, 2 mmol/L tetrasodium pyrophosphate, 20 mmol/L Tris, 1 % Triton® X-100, 20 mmol/L sodium glycerophosphate, 10 mmol/L sodium fluoride, 2 mmol/L sodium vanadate, 1 mmol/L PMSF, 1× Complete). Samples were centrifuged at 11 180r/min and 4 °C for 10 min and aliquots of the supernatant were used for the determination of protein concentration by the bicinchoninic acid assay method[41]. Equal amounts

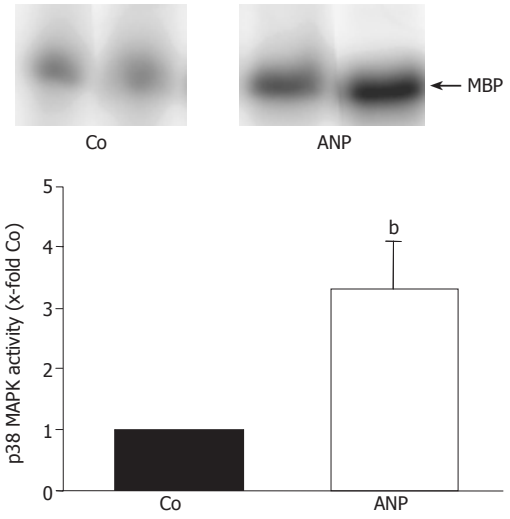

Figure 1 Effect of ANP pretreatment on p38 MAPK activity. After intravenous infusion of ANP (5 μg/kg) or NaCl (Co) for 20 min livers were snap-frozen and homogenized in lysis buffer. Following immunoprecipitation, the assay was performed as described in "Materials and methods", and samples were separated by SDS-PAGE. One representative kinase activity assay specific for p38 MAPK is shown with $n = 2$ (out of $n = 4$) for each treatment group. p38 MAPK activity in the liver homogenates is presented as 10-fold control (30-min perfusion), and is expressed as mean±SE of $n = 4$ experiments in each treatment group. $^{b}P<0.01$ *vs* control.

of protein were incubated with 1.5 μL of anti-p38 antibody shaking for 2 h. Afterwards immunoprecipitation was performed with 15 μL protein A agarose shaking overnight at 4 °C. Samples were centrifuged at 11 180×*g* (4 °C, 10 min) and pellets were washed thrice with lysis buffer and once with kinase buffer (20 mmol/L Hepes pH 7.5, 20 mmol/L $MgCl_2$, 25 mmol/L sodium glycerophosphate, 100 μmol/L sodium vanadate, 2 mmol/L DTT). Precipitates were resuspended in 20 μL kinase buffer, before 3 μL substrate solution (1 mg/mL of recombinant MBP, Sigma, Deisenhofen, Germany) and 10 μL of an ATP mix were added, the latter containing kinase buffer with 10 mCi/mL [γ^{32}P]-ATP, (3 000 Ci/mmol, Amersham, Braunschweig, Germany), 5 mmol/L ATP and 2 mol/L $MgCl_2$. The reaction mixture was then incubated for 20 min at 30 °C shaking. Phosphorylation was stopped by adding 6 μL 5× Laemmli buffer and heating for 3 min at 90 °C. Samples were separated by SDS-PAGE and band intensities quantified by phosphor-imaging (Packard, Meriden, USA). The ratio of digital light units (DLU) of respective values *vs* controls was determined.

Statistical analysis

All experiments were performed at least thrice per treatment group (5 animals per treatment). Results were expressed as mean±SE (n = number of organs). Statistical significance between the groups was determined with one sample or Student's t-test using GraphPad Prism® Version 3.02 for Windows (GraphPad Software Inc., San Diego, USA). $P<0.05$ were considered statistically significant.

RESULTS

ANP pretreatment causes increased p38 MAPK activity

In order to confirm our previous findings that preconditioning with ANP increases p38 MAPK activity in the liver[8], rats were treated intravenously with 200 nmol/L ANP or NaCl and livers were excised and homogenized in lysis buffer. Homogenates were analyzed by *in vitro* phosphorylation assay to determine the activity of p38 MAPK. As shown in Figure 1, hepatic p38 MAPK activity in livers of ANP-preconditioned rats was significantly increased compared to NaCl treated animals. These data confirm the stimulatory effect of ANP on p38 MAPK *in vivo,* with increased p38 MAPK activity after 20 min perfusion representing an early signaling event in ANP preconditioning.

ANP preconditioning leads to increased F-actin content after ischemia

As an activation of p38 MAPK has been shown to be connected with alterations of the cytoskeleton in other cells and organ systems, we investigated the polymerization state of actin in untreated *vs* ANP-perfused livers. Liver tissue was fractionated into a cytosolic (G-actin) and a cytoskeletal (F-actin) fraction in order to discriminate between the hepatic content of G- and F-actin, respectively. In untreated livers, F-actin content did not change during ischemia and reperfusion (Figures 2A and B). In contrast, ANP-preconditioned livers exhibited an obvious augmentation of F-actin after 24 h ischemia accompanied by a decrease in hepatic G-actin, which prolonged during reperfusion (Figures 2A and B). Neither I/R nor ANP preconditioning altered total hepatic actin content. This was examined by homogenizing liver tissue and analyzing samples by Western blotting without prior fractionation (Figures 2C and D).

Perfusion with SB203580 abrogates ANP-mediated increase of hepatocyte F-actin

In order to study the correlation between activation of p38 MAPK and cytoskeletal changes in untreated and ANP-preconditioned livers, we used the specific p38 MAPK inhibitor SB203580. Perfusion with 2 μmol/L SB203580 together with ANP completely abolished the enhanced hepatic F-actin content after ANP preconditioning (Figure 3A). Similarly, inhibition of p38 MAPK by SB203580 abrogated the decrease of G-actin in ANP pretreated liver homogenates, so that G-actin content in these samples resembled untreated controls (Figure 3B). Perfusion with the inhibitor alone did not affect the distribution of cytosolic G- and cytoskeletal F-actin in the liver (Figures 3A and B).

Changes in F-actin by ANP detected by Western blot analysis were confirmed by staining of tissue sections. Staining with rhodamine-conjugated phalloidin, which specifically binds to F-actin, showed a low fluorescence in tissue sections of untreated livers, which correlated with a marginal F-actin content (Figure 4A). Pretreatment

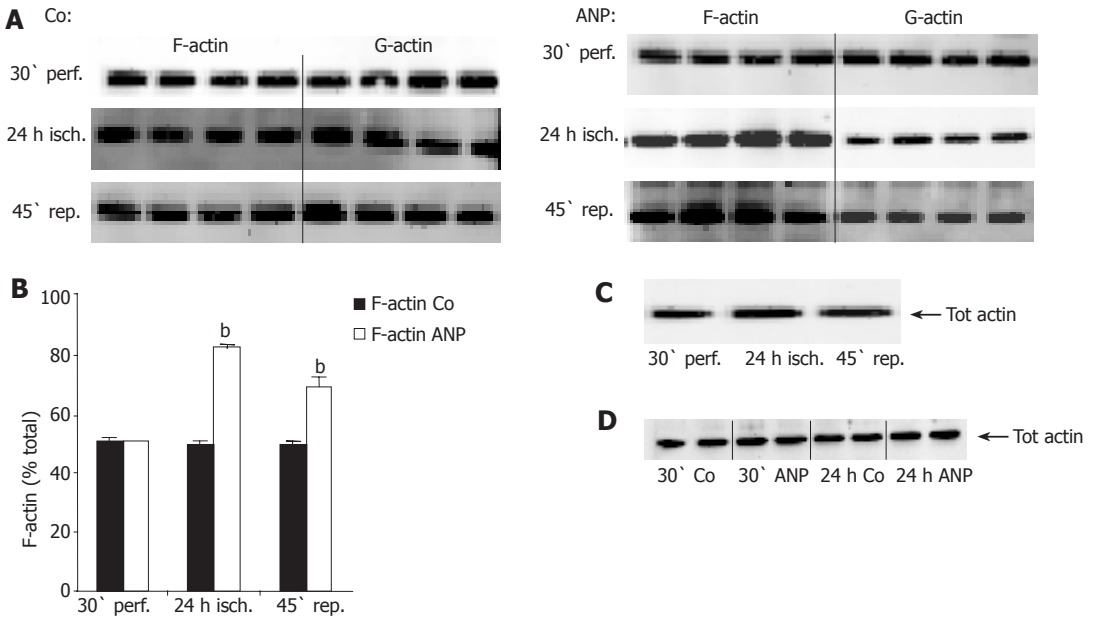

Figure 2 Influence of ANP preconditioning and ischemia on total actin and F-actin content. Livers were perfused for 30 min in the absence or presence of 200 nmol/L ANP, which was added 20 min prior to ischemia. Afterwards, livers were kept under ischemic conditions for 24 h (4 °C) in UW solution. At the indicated times, livers were snap-frozen, homogenized, and analyzed by Western blot using an anti-actin antibody. For differentiation between F- and G-actin (cytoskeleton and cytosol, respectively), liver homogenates were fractionated before Western blot analysis according to "Materials and methods" (**A** and **B**). One representative Western blot is imaged for each experimental setting. (**A**) Western blots representing hepatic F- and G-actin content during IR in untreated (Co) and ANP-preconditioned livers after 30-min perfusion (30' perf.), 24-h ischemia (24-h isch.), and 45-min reperfusion (45' rep.). (**B**) Quantitative/densitometric analysis of F- and G-actin content during IR in untreated (Co) or ANP-preconditioned livers. Data are expressed as percent of total actin content (F-actin+G-actin=100%) as mean±SE of n = 4 experiments in each treatment group. $^{b}P<0.001$ *vs* appropriate control. (**C**) Western blot showing total actin in untreated liver homogenates after 30-min perfusion, 24-h ischemia, and 45-min reperfusion. (**D**) Total hepatic actin content after perfusion (30') and ischemia (24-h) in ANP treated or untreated (Co) livers detected by Western blot analysis.

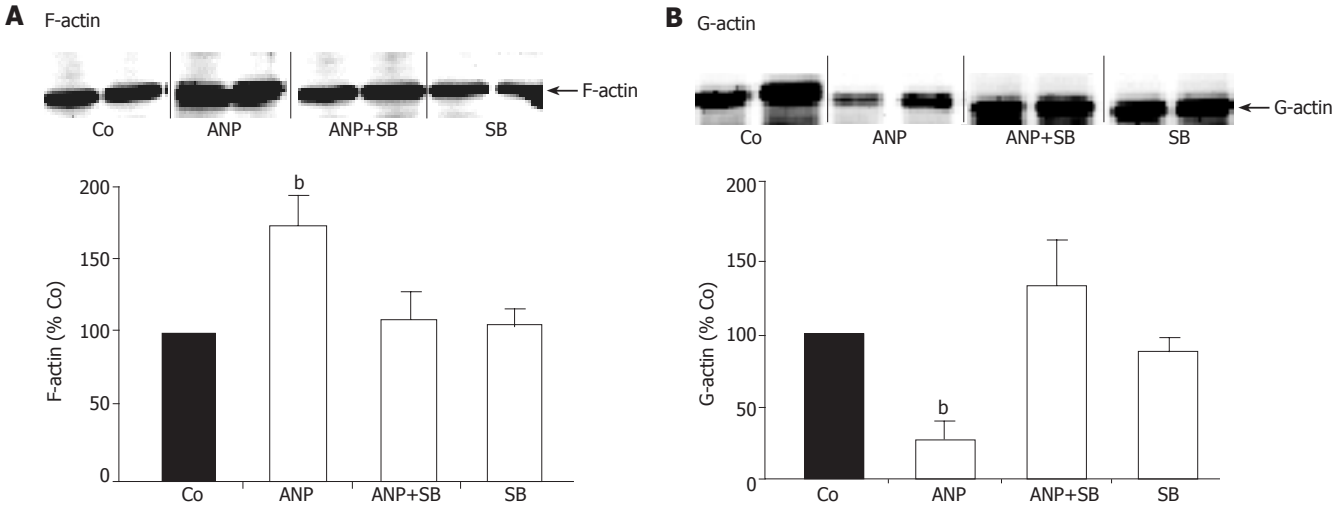

Figure 3 Effect of p38 MAPK inhibition on distribution of F- and G-actin. 20 min prior to ischemia livers were preconditioned with 200 nmol/L ANP or left untreated (Co) followed by 24-h ischemia at 4 °C. In different experiments, livers were perfused with SB203580 (2 μmol/L) or with a combination of SB203580 (2 μmol/L) and ANP (200 nmol/L). After ischemia livers were snap-frozen, homogenized and divided into cytoskeletal (**A**) and cytosolic (**B**) fraction by fractionation as described above. Samples were analyzed by Western blotting using an anti-actin antibody for detection of F-actin (**A**) in the cytoskeletal fraction and G-actin (**B**) in the cytosolic fraction. One representative Western blot is shown for each fraction. Bars show percentage of hepatic F-actin (**A**) or G-actin (**B**) in ANP, ANP+SB203580 and SB203580 treated livers referring to untreated control livers. Results are expressed as mean±SE of n = 4 experiments in each treatment group. $^{b}P<0.01$ *vs* control after 24-h ischemia.

with ANP caused very intensive staining of liver slices, representing an obvious increase in hepatic F-actin content (Figure 4B).

When stained with rhodamine-conjugated phalloidin, slices of ANP pretreated livers showed very intensive staining, representing an obvious increase in hepatic F-actin content especially at apical membranes of hepatocytes (Figure 4B) confirming the results obtained by Western blot analysis. Again, perfusion of the livers with SB203580 abolished the effect of ANP preconditioning on

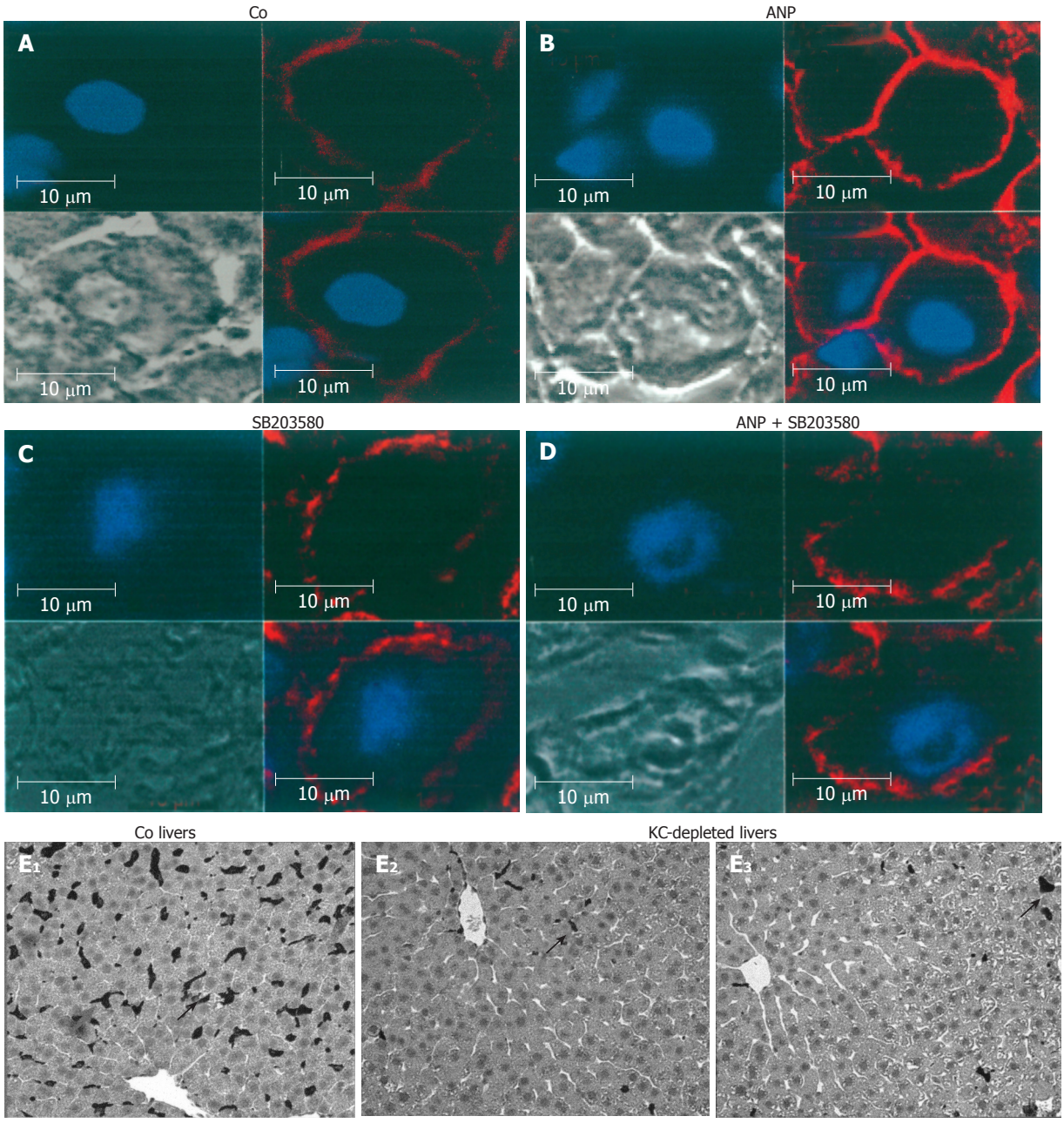

Figure 4 Analysis of the influence of ANP preconditioning on localization of F-actin in the liver by confocal microscopy. Livers were left untreated (**A**): preconditioned with 200 nmol/L ANP (**B**): 2 μmol/L SB203580 (**C**): or perfused with a combination of ANP (200 nmol/L) and SB203580 (2 μmol/L) (**D**): After ischemia (24 h, 4 °C), livers were snap-frozen, cut into 6-μm slices and stained with rhodamine-conjugated phalloidin (red, F-actin) and Hoechst 33342 (blue, nuclei) as described in "Materials and methods". Liver sections were observed by confocal laser microscopy (63-fold amplification). Immunohistological staining of KCs in untreated (Co) and KC-depleted livers (**E**): rats received an intravenous injection of 900 μL NaCl (Co) or 900 μL liposomes (12 mmol/L Cl_2MBP) into the tail vein. After 48 h rat livers were perfused, snap-frozen and liver slices were stained with an antibody against the KC-specific surface marker ED2 (see "Methods") to verify the Cl_2MBP-dependent depletion of the KCs. Dark staining represents KC (hallmarked with arrows). (**F**): KCs were depleted with Cl_2MBP as described under "Methods". After 48 h control organs (Co) or KC-depleted livers (12 mmol/L Cl_2MBP) were perfused ±ANP (200 nmol/L) for 20 min. Then p38 MAPK activity was investigated by *in vitro* phosphorylation assay (see "Methods"). Determination of density light units was performed by phosphorimaging and values of ANP-pretreated cells were divided by mean values of the respective control group. Columns show mean±SE of 4-5 independent perfusion experiments with $^bP<0.01$ being statistically different from the respective control group.

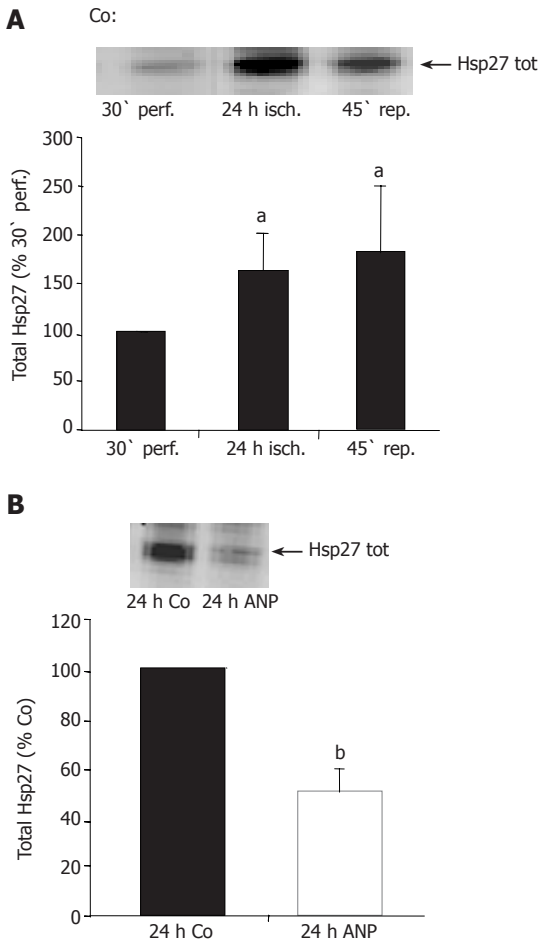

Figure 5 Changes in hepatic total Hsp27 during ischemia – influence of ANP pretreatment. Livers were perfused for 30 min in the presence or absence of ANP followed by 24-h ischemia at 4 °C in UW solution and reperfusion for 45 min. Afterwards, livers were snap-frozen at the indicated times, homogenized and analyzed via Western blot using an anti-Hsp27 antibody for detection of total Hsp27. One representative Western blot is shown for each experimental setting (untreated controls: (**A**), ANP pretreated livers: (**B**)). (**A**) Effect of IR on total Hsp27 in the liver. The graph shows percentage of values for untreated livers (Co) after 30-min perfusion (30' perf.) as means±SE of $n = 4$ experiments in each group. [a]$P<0.05$ *vs* untreated control after 30-min perfusion. (**B**) Influence of ANP preconditioning on total Hsp 27 after 24-h ischemia. Bars represent total Hsp27 as % Co after 24-h ischemia. Data are expressed as means±SE of $n = 4$ experiments in each treatment group. [b]$P<0.01$ *vs* control after 24-h ischemia.

F-actin, as it yielded a marginal staining intensity matching the intensity of untreated livers (Figure 4D), linking the effect to an activation of p38 MAPK.

Confocal data showed that changes in hepatic cytoskeleton occurred in parenchymal cells. The localization of p38 MAPK activation, however, has yet to be determined. We, therefore, measured p38 MAPK activation in both isolated Kupffer cells as well as in isolated hepatocytes. This experiment revealed no activation of p38 MAPK upon ANP treatment in KC, but a significant activation in hepatocytes (data not shown). Since the extent of activation was lower than that observed in whole livers[8] and since ANP has been reported as a regulator of Kupffer cell functions[43], we hypothesized that activation might occur in whole livers as a paracrine effect of Kupffer cells on hepatocytes.

To verify this potential cell interaction, we investigated the ANP-mediated effect on p38 MAPK in KC-depleted livers. For this purpose, we first audited the Cl_2MBP-dependent KC depletion via immunohistological staining of the macrophages with ED2 antibody (Figure 4E). In fact, Cl_2MBP led to a depletion of the KCs compared to NaCl-treated livers (Figure 4F). Furthermore, LDH efflux into the perfusate was determined to exclude Cl_2MBP-induced liver damage. The measurement indicated no increase in LDH-activity and thus no liver toxicity of Cl_2MBP (data not shown).

Subsequently, ANP-induced p38 MAPK activity was measured by determination of the radioactive labeled kinase substrate MBP. Surprisingly, liver perfusion with ANP exhibited no differences in kinase activity in KC-depleted or non-depleted livers (Figure 4F). Due to this observation we suggest that ANP mediates p38 MAPK activation not via hepatocyte-KC interaction.

Changes of total Hsp27 content and translocation of the heat shock protein

As the small heat shock protein Hsp27 has been demonstrated to be an important downstream target of p38 MAPK, which plays a critical role in the regulation of F-actin polymerization in different systems, we focused on a possible influence of ischemia on the expression of Hsp27 in the liver. Liver homogenates were analyzed by Western blot analysis without prior fractionation in order to investigate the hepatic content of total Hsp27. At the end of ischemia, Hsp27 levels in untreated livers were significantly higher than after 30-min perfusion (Figure 5A). This increase persisted during 45 min reperfusion.

To prove whether changes in total Hsp27 content are accompanied by a translocation of the heat shock protein towards the cytoskeleton, as described in previous studies[31,32], we investigated its subcellular distribution in liver tissue after ischemia. Liver tissue was fractionated, Hsp27 content in the cytosolic and cytoskeletal fraction was determined by Western blot analysis, and band intensity was considered proportional to the content of Hsp27 in the respective fraction. We were able to demonstrate that ischemia caused a translocation of the heat shock protein towards the cytoskeleton, as the content of total Hsp27 in cytoskeletal fractions accelerated after 24 h ischemia (Figure 6A). At this time more than 80% of the heat shock protein was localized in the cytoskeletal fraction of untreated liver homogenates (Figures 6A and B). This translocation seemed to decline during reperfusion (Figure 6A).

Interestingly, Western blot analysis of the whole tissue samples revealed that after 24 h ischemia ANP-pretreated livers showed significantly lower levels of total Hsp27 compared to untreated samples (Figure 5B). Surprisingly, the translocation of the heat shock protein detected in control livers was completely missing, so that the content of total Hsp27 in cytoskeletal and cytosolic fraction after ischemia was very similar (Figure 6B). Thus, pretreatment with ANP apparently both attenuates Hsp27 protein rise induced by I/R and prevents the translocation of Hsp27 to the cytoskeleton after ischemia.

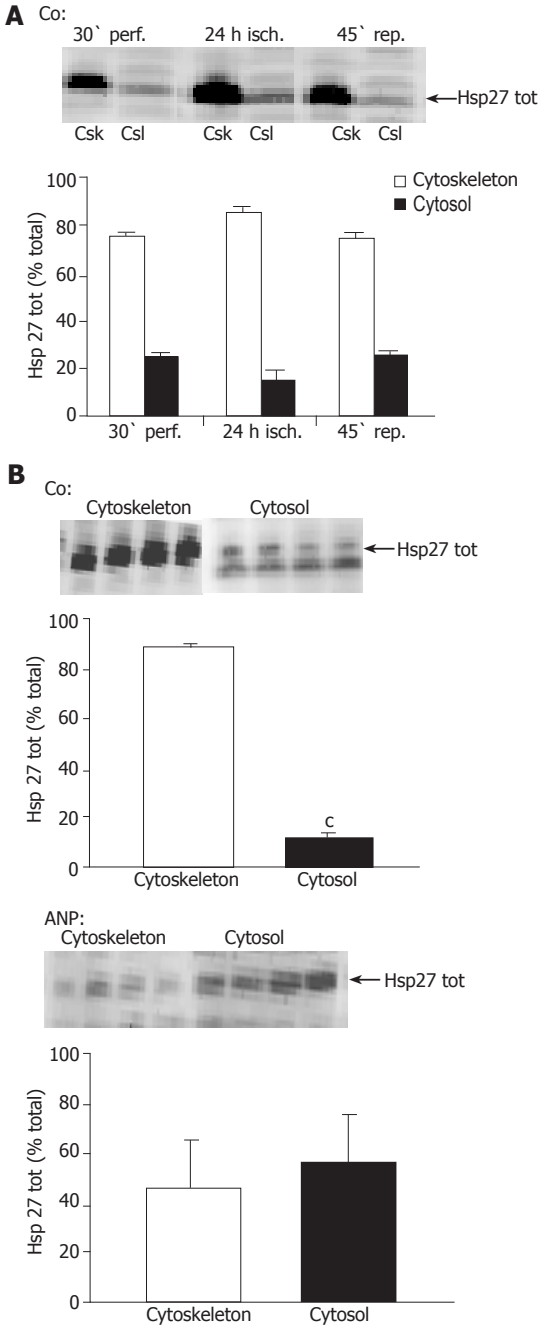

Figure 6 Influence of ischemia and ANP pretreatment on Hsp27 distribution. After perfusion for 30 min in the absence (**A** and **B**) or presence (**B**) of ANP, 24-h ischemia in cold UW solution, and reperfusion for 45 min, livers were snap-frozen, homogenized and fractionated as described in "Materials and methods". Samples were taken at indicated times and total Hsp27 in cytoskeletal (Csk) and cytosolic (Csl) fraction was detected via Western blot analysis using an anti-Hsp27 antibody. One representative Western blot is shown for each treatment group. (**A**) Effect of ischemia and reperfusion on the distribution of total Hsp27 in the liver. Quantification of total Hsp27 in the liver samples was verified via densitometric analysis of the corresponding bands, which was used to evaluate the ratio of Hsp27 in the cytoskeletal fraction (Csk) resp. cytosolic fraction (Csl) referring to total Hsp27 signal (cytoskeleton+cytosol) in the respective sample. Data are expressed as percent of total Hsp27 in cytoskeletal (F-actin) and cytosolic (G-actin) fraction as mean±SE of n=4 experiments in each treatment group. [a]P<0.05, *vs* Hsp27 content in cytoskeletal fraction in untreated livers after 30-min perfusion. (**B**) Distribution of total Hsp27 in untreated (control) and ANP-preconditioned livers after 24-h ischemia. Results are shown as percent of total Hsp27 in cytosolic and cytoskeletal fraction. Data are presented as mean±SE of n=4 experiments in each treatment group. [c]P<0.001 *vs* Hsp27 content in cytoskeletal fraction of untreated livers after 24-h ischemia. In ANP treated livers the differences in the values were not significant.

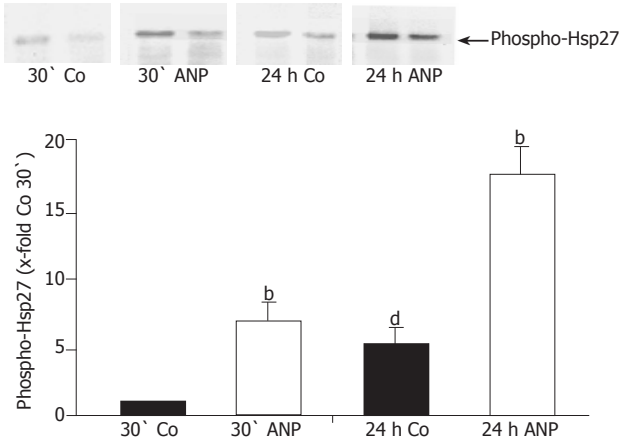

Figure 7 Influence of pretreatment with ANP on phosphorylation status of Hsp27. After perfusion for 10 min with KH-buffer livers were preconditioned with ANP for 20 min or left untreated, followed by 24-h ischemia (4 °C) according to the study protocol. Samples were taken after 30-min perfusion and 24-h ischemia. Livers were snap-frozen and homogenized, followed by immunoprecipitation with an anti-Hsp27 antibody and Western blot analysis using an anti-phospho-Hsp27 antibody. One representative Western blot is shown. Content of phospho-Hsp27 in the liver homogenates is presented as 10-fold control after 30-min perfusion, using the respective control as reference value and expressed as mean±SE of n = 4 experiments in each treatment group. Statistical analysis of ANP pretreated samples: [b]P<0.001 *vs* phospho-Hsp27 in respective control (after 30-min perfusion or 24-h ischemia). Statistical analysis of untreated control samples: [d]P<0.01 *vs* phospho-Hsp27 in control after 30-min perfusion.

ANP preconditioning causes increased phosphorylation of Hsp27

The influence of Hsp27 on actin polymerization depends on its phosphorylation status. Hence it was important to analyze the effect of ischemia and ANP preconditioning on the phosphorylation status of Hsp27. Detecting phospho-Hsp27 by Western blot analysis we obtained a significant increase of phosphorylation of the heat shock protein after ischemia in homogenates of untreated livers (Figure 7). In ANP-preconditioned samples phosphorylation seen after 30-min perfusion was already more intense than in untreated livers but increased even more after 24 h ischemia. Resuming these results, ANP seems to enhance the phosphorylation status of Hsp27 after 30-min perfusion and 24-h ischemia (Figure 7).

Inhibition of p38 MAPK prevents phosphorylation of Hsp27 in ANP pretreated livers

Pretreatment with ANP leads to an enhanced activation of p38 MAPK both in the isolated perfused liver as well as *in vivo* (Ref.[8] and Figure 1). We, therefore, investigated a possible connection between p38 MAPK activation and phosphorylation of its downstream target Hsp27 by using the specific p38 MAPK inhibitor SB203580. This treatment in fact completely abrogated the increase of Hsp27 phosphorylation induced by ANP (Figure 8). Pretreatment with SB203580 alone exerted no significant effect on phosphorylation of Hsp27 (Figure 8). Thus, activation of p38 MAPK is essential for the phosphorylation of the heat shock protein.

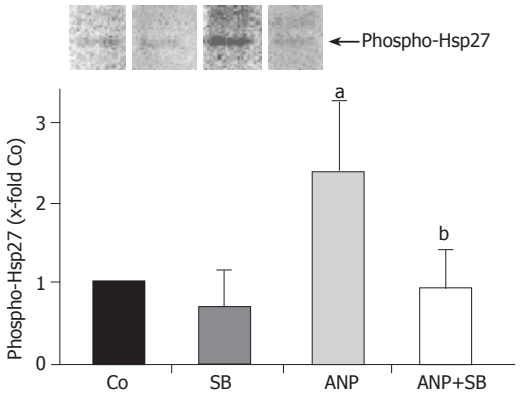

Figure 8 Effect of p38 MAPK inhibition on phosphorylation status of Hsp27. Livers were perfused for 30 min in the absence (Co) or presence of 200 nmol/L ANP, which was added 20 min prior to 24-h ischemia (4 °C). In different experiments, livers were perfused for 20 min with SB203580 (2 μmol/L) or with a combination of SB203580 (2 μmol/L) and ANP (200 nmol/L). After ischemia, livers were snap-frozen and homogenized. Total Hsp27 was precipitated as described and the content of phosphorylated Hsp27 was determined by Western blotting and detection with anti-phospho-Hsp27 primary antibody. One representative Western blot is shown. In the graph hepatic content of phospho-Hsp27 is expressed as percent of control samples after 24-h ischemia as mean±SE of n = 4 experiments in each treatment group. [a]P<0.05 *vs* control after 24-h ischemia, [b]P<0.01 *vs* phospho-Hsp27 content in ANP pretreated livers.

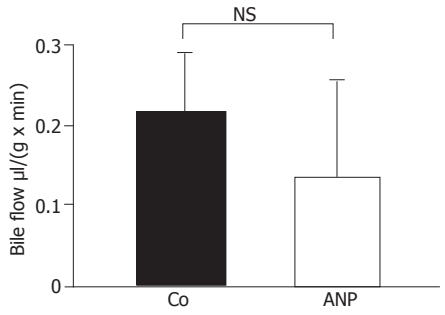

Figure 9 Effect of ANP preconditioning on bile flow. Bile was collected during perfusion and reperfusion and quantified volumetrically. Bile flow is expressed as μL per min and g liver tissue. Results show mean±SE of n = 4 experiments in each treatment group. The differences between untreated (Co) and ANP-preconditioned group were not significant.

ANP preconditioning shows no effect on bile flow

The cytoskeleton, more precisely F-actin, plays an important role in the maintenance of liver function[14,18,19]. In order to investigate a functional significance of an increase in F-actin after treatment with ANP, we studied the bile flow in transplanted organs of ANP- and NaCl-treated rats. Bile was collected as described during infusion and reperfusion. As shown in Figure 9, no significant differences between livers from NaCl-treated and from ANP-preconditioned rats could be detected. Thus, ANP-mediated increase of hepatic F-actin content does not cause an improvement of bile flow after ischemia.

DISCUSSION

This paper provides an important insight into the changes in hepatic cytoskeletal structures during I/R, signaling mechanisms in their modulation, and the interference of ANP preconditioning with these mechanisms.

Besides its vasodilating, hypotensive, and natriuretic activities[44], ANP has been described to protect against IRI *ex vivo* in the liver and *in vivo* in the heart[7,5,8,45], and to strongly activate p38 MAPK[8]. Interestingly, this activation has no influence on ANP's potential to protect from hepatic cell death, as previously shown by Kulhanek-Heinze *et al*[13]. In the present work, we therefore aimed to elucidate other potential functional consequences of ANP-induced p38 MAPK activity. In this context, we were able to demonstrate a clear coherence between ANP-mediated activation of p38 MAPK in the liver after ischemia and structural changes of the hepatocyte cytoskeleton. Interestingly, however, no functional correlation to improved bile flow could be established.

Cytoskeleton of hepatocytes during IR

Due to the evidence that activation of p38 MAPK leads to cytoskeletal changes in other systems[46] and the lack of knowledge about similar pathways in the liver, we investigated cytoskeletal changes during IR. We were able to show that hepatic content of total actin was affected neither by IR alone nor in combination with preconditioning of livers with ANP. Surprisingly, F-actin levels were not impaired by ischemia in control tissue after I/R. This result does not correspond to the findings of Cutrin *et al*[47]. who demonstrated structural changes of actin filaments after cold ischemia (120 min) and particularly after reperfusion (60-90 min) in transplanted human livers. Besides different species that were investigated, especially the much longer ischemic period employed in our model might account for these differences. In the kidney, Schwartz *et al*[30]. found a distinct increase of G-actin, paralleled by apical actin disruption after 30 min of warm ischemia. Again, the length, and also the temperature of ischemia cannot be compared to our experimental settings. Moreover, mechanisms in the kidney might differ from that in the livers. To the best of our knowledge, our data for the first time describe no significant cytoskeletal alterations in rat livers after prolonged hypothermic storage.

Cytoskeletal changes in ANP pretreated livers

Recently Gomes *et al*[28]. proved that IPC preserves rat kidneys from IRI by upregulation of genes coding for cytoskeletal proteins. The demonstrated increase in mRNA of these proteins, which have an F-actin-stabilizing function, is discussed to contribute to the tolerance of preconditioned tissue to ischemia. This effect, which was observed already after 30 min of preconditioning, goes along with our findings of an augmentation of F-actin in ANP-preconditioned livers confirming the influence of protective preconditioning (IPC or ANP pretreatment) on F-actin content of the affected tissue. Based on the findings that ANP preconditioning as well as IPC protects against IRI and due to the importance of F-actin for regulating cell morphology, intracellular processes, and bile secretion in liver cells, we hypothesized

that an augmentation of hepatic F-actin after ischemia might be a feature of the cytoprotective activities of ANP. Interestingly, however, although F-actin content increased in pretreated organs, we found no improvement of bile flow. Therefore, other functional parameters depending on the demonstrated F-actin formation in ANP pretreated livers need to be further investigated.

Involvement of p38 MAPK

As there are no data concerning a possible connection between p38 MAPK activation and cytoskeletal changes in liver tissue, we focused on the effect of p38 MAPK inhibition on hepatic F-actin content after ANP pretreatment. We applied the p38 MAPK inhibitor SB203580 at a concentration of 2 μmol/L to assure its specificity[48]. We demonstrated that perfusion with the inhibitor alone does not cause any cytoskeletal changes in liver tissue, but completely abolishes the ANP-induced effect of increased F-actin content in pretreated livers. Thus, we showed for the first time that ANP-mediated p38 MAPK activation leads to hepatic cytoskeletal changes by increasing the hepatocyte F-actin content in rat livers. To investigate a possible paracrine effect of KC on hepatocytes, p38 MAPK activity was determined in KC-depleted livers. Since KC depletion did not alter the activation of p38 MAPK, we suggest that an interaction between hepatocytes and KCs is not involved in ANP-mediated p38 MAPK activation.

Changes in total Hsp27

Analyzing total Hsp27 protein levels, we were able to show that the hepatic content of total Hsp27 increases during ischemia. It is a known fact that Hsp27 accumulates after cellular stress like hyperthermia[36], but also bacterial lipopolysaccharide (LPS) and Cyclosporine A enhance Hsp27 levels[49,50]. Thus, cellular stress can lead to an increase of Hsp27 content in the affected tissue elucidating the augmentation of the heat shock protein in the liver, which we observed during ischemia in untreated livers. This increased expression of the heat shock protein has been discussed to be a protective response, as it provides prevention from simulated IRI in canine myocytes[51]. Although our results of an augmentation of Hsp27 expression during ischemia, representing a situation of cellular stress, confirm these published data, our findings are surprising, as energy-dependent processes such as protein synthesis seem rather unlikely at 4 °C during a period of 24 h. Interestingly, however, such incidents have been observed before: Gerwig *et al*[6]. demonstrated an increase of caspase-3 precursor CPP 32 during an ischemic period and Wilhelm *et al*[52]. proved that cold ischemia induces upregulation of endothelin-1 in the kidney.

Detection of total Hsp27 in ANP-pretreated livers, however, yielded a rather astonishing result, as these organs showed markedly decreased levels of the heat shock protein. Interestingly, an increase of Hsp27 after cellular stress and decrease of the heat shock protein after treatment with a substance possessing protective properties has been described before for the kidney by Stacchiotti *et al*[50]. Hsp27 overexpression was seen after oxidative stress but disappeared after administration of an antioxidant[50]. This effect was ascribed to the cytoprotective effect of the antioxidant, which made additional protective Hsp27 response unnecessary. As ANP has been shown to protect against IRI[7,5], the effects seen in pretreated livers could be similar to the results of Stacchiotti *et al*. Thus, ANP might contribute to a protection of the liver tissue, so that higher levels of total Hsp27 as an additional protective response are no longer necessary.

It has to be noted that the functional consequences of changes in Hsp27 expression largely depend on its phosphorylation status and on its subcellular distribution, which will be subsequently discussed.

Translocation of total Hsp27

Sakamoto *et al*[34]. demonstrated that in rat hearts ischemia induces translocation of Hsp27 to the cytoskeleton and Aufricht *et al*[26]. showed the same effect in rat kidneys. Therefore, we investigated the subcellular distribution of the heat shock protein in isolated perfused rat livers after ischemia. In fact, significant augmentation of total Hsp27 in the cytoskeletal liver fraction could be detected after 24 h ischemia, suggesting a translocation of the heat shock protein towards the cytoskeleton. Pretreatment with ANP, however, completely abolished translocation of Hsp27 after ischemia. This observation enforces the assumption that ANP radically alters the response of liver cells to ischemia in isolated rat livers.

Phosphorylation status of Hsp27

As functional consequences of changes in Hsp27 protein expression and subcellular distribution largely depend on the phosphorylation status of the heat shock protein, we focused on this parameter next.

We proved that ischemic conditions cause phosphorylation of Hsp27 in isolated perfused rat liver, confirming the results of Huot *et al*[53]. who demonstrated an increased content of phosphorylated Hsp27 in vascular endothelial cells after oxidative stress. As the heat shock protein in its phosphorylated form is able to enhance F-actin formation, we expected a higher F-actin content in livers after ischemia. Interestingly, we could not detect an increase in hepatic F-actin in these organs. Since the augmentation of phosphorylation in untreated livers was not excessively high, the resulting effect on the cytoskeleton might not be sufficient to induce F-actin formation in liver tissue after ischemia.

In contrast, pretreatment with ANP resulted in a much stronger increase of the phosphorylation of the heat shock protein, which could be seen already after perfusion and obviously accelerated during ischemia (up to almost 20-fold of untreated controls). These findings correlate with data presented by Sanada *et al*[12]. showing changes in the phosphorylation status of Hsp27 after protective pretreatment of organs before ischemia *in vivo* in terms of an increased phosphorylation of the heat shock protein

after IPC. As Sanada *et al*. furthermore demonstrated coherence between Hsp27 phosphorylation and activation of p38 MAPK, we investigated this possible connection by perfusion of the livers with SB203580 in combination with ANP. An inhibition of p38 MAPK reduced the phosphorylation status of Hsp27 to basal levels. Thus, our results clearly prove the dependency of Hsp27-phosphorylation in the liver on prior activation of p38 MAPK.

Alterations of the cytoskeleton, particularly of F-actin content, are often discussed as a consequence of changes in the phosphorylation status of Hsp27 in other cell/organ systems[54]. We were able to confirm for the first time this correlation in the liver by showing an ANP-mediated increase of Hsp27 phosphorylation, which results in an accumulation of hepatic F-actin after ischemia. This effect is mediated via p38 MAPK, as an increase of F-actin in the liver after ANP preconditioning was abrogated by the p38 MAPK inhibitor SB203580.

Higher hepatic F-actin levels are thought to stabilize the cytoskeleton and to improve contractility resulting in improved bile flow after ischemia[15]. Our own data, however, do not show improved bile flow upon ANP pretreatment. Functional parameters other than improved bile flow are therefore hypothesized to be mediated by cytoskeletal changes, which need further investigation.

In summary, we were able to show for the first time the dependency of F-actin content in the liver on activation of p38 MAPK and that ANP preconditioning mediates changes in the cytoskeleton via an activation of p38 MAPK and phosphorylation of Hsp27 in the liver.

ACKNOWLEDGMENTS

We thank Dr. Stefan Zahler for his excellent support in confocal microscopy and processing of images, Kathrin Ladezki-Baehs for determination of p38 MAPK activity, and Dr. H. Meißner and Andrea Sendelhofert (both Institute of Pathology, University of Munich, Germany) for performing immunostaining. Clodronate was a gift of Roche Diagnostics GmbH, Mannheim, Germany.

REFERENCES

1 **Bilzer M,** Gerbes AL. Preservation injury of the liver: mechanisms and novel therapeutic strategies. *J Hepatol* 2000; **32**: 508-515
2 **Jaeschke H**. Molecular mechanisms of hepatic ischemia-reperfusion injury and preconditioning. *Am J Physiol Gastrointest Liver Physiol* 2003; **284**: G15-G26
3 **Kang KJ**. Mechanism of hepatic ischemia/reperfusion injury and protection against reperfusion injury. *Transplant Proc* 2002; **34**: 2659-2661
4 **Bilzer M,** Witthaut R, Paumgartner G, Gerbes A**L**. Prevention of ischemia/reperfusion injury in the rat liver by atrial natriuretic peptide. *Gastroenterology* 1994; **106**: 143-151
5 **Gerbes AL,** Vollmar AM, Kiemer AK, Bilzer M. The guanylate cyclase-coupled natriuretic peptide receptor: a new target for prevention of cold ischemia-reperfusion damage of the rat liver. *Hepatology* 1998; **28**: 1309-1317
6 **Gerwig T,** Meissner H, Bilzer M, Kiemer AK, Arnholdt H, Vollmar AM, Gerbes AL. Atrial natriuretic peptide preconditioning protects against hepatic preservation injury by attenuating necrotic and apoptotic cell death. *J Hepatol* 2003; **39**: 341-348
7 **Cottart CH,** Nivet-Antoine V, Do L, Al-Massarani G, Descamps G, Xavier-Galen F, Clot JP. Hepatic cytoprotection by nitric oxide and the cGMP pathway after ischaemia-reperfusion in the rat. *Nitric Oxide* 2003; **9**: 57-63
8 **Kiemer AK,** Kulhanek-Heinze S, Gerwig T, Gerbes AL, Vollmar AM. Stimulation of p38 MAPK by hormonal preconditioning with atrial natriuretic peptide. *World J Gastroenterol* 2002; **8**: 707-711
9 **Schauer RJ,** Gerbes AL, Vonier D, op den Winkel M, Fraunberger P, Bilzer M. Induction of cellular resistance against Kupffer cell-derived oxidant stress: a novel concept of hepatoprotection by ischemic preconditioning. *Hepatology* 2003; **37**: 286-295
10 **Teoh N,** Dela Pena A, Farrell G. Hepatic ischemic preconditioning in mice is associated with activation of NF-kappaB, p38 kinase, and cell cycle entry. *Hepatology* 2002; **36**: 94-102
11 **Nakano A,** Baines CP, Kim SO, Pelech SL, Downey JM, Cohen MV, Critz SD. Ischemic preconditioning activates MAPKAPK2 in the isolated rabbit heart: evidence for involvement of p38 MAPK. *Circ Res* 2000; **86**: 144-151
12 **Sanada S,** Kitakaze M, Papst PJ, Hatanaka K, Asanuma H, Aki T, Shinozaki Y, Ogita H, Node K, Takashima S, Asakura M, Yamada J, Fukushima T, Ogai A, Kuzuya T, Mori H, Terada N, Yoshida K, Hori M. Role of phasic dynamism of p38 mitogen-activated protein kinase activation in ischemic preconditioning of the canine heart. *Circ Res* 2001; **88**: 175-180
13 **Kulhanek-Heinze S,** Gerbes AL, Gerwig T, Vollmar AM, Kiemer AK. Protein kinase A dependent signalling mediates anti-apoptotic effects of the atrial natriuretic peptide in ischemic livers. *J Hepatol* 2004; **41**: 414-420
14 **Denk H,** Lackinger E, Vennigerholz F. Pathology of the cytoskeleton of hepatocytes. *Prog Liver Dis* 1986; **8**: 237-251
15 **Rungger-Brändle E, Gabbiani G**. The role of cytoskeletal and cytocontractile elements in pathologic processes. *Am J Pathol* 1983; **110**: 361-392 [PMID: 6219586]
16 **Selzner N,** Rüdiger H, Graf R, Clavien PA. Protective strategies against ischemic injury of the liver. *Gastroenterology* 2003; **125**: 917-936
17 **Feldmann G**. The cytoskeleton of the hepatocyte. Structure and functions. *J Hepatol* 1989; **8**: 380-386
18 **Fisher MM,** Phillips MJ. Cytoskeleton of the hepatocyte. *Prog Liver Dis* 1979; **6**: 105-121
19 **Marceau N,** Loranger A, Gilbert S, Daigle N, Champetier S. Keratin-mediated resistance to stress and apoptosis in simple epithelial cells in relation to health and disease. *Biochem Cell Biol* 2001; **79**: 543-555
20 **Ohashi M,** Sano N, Takikawa H. Effects of phalloidin on the biliary excretion of cholephilic compounds in rats. *Pharmacology* 2002; **66**: 31-35
21 **Arias I.M.** The Liver: Biology and Pathobiology. Raven Press, Ltd, New York 2001; Book Chapter
22 **Song JY,** Van Marle J, Van Noorden CJ, Frederiks WM. Disturbed structural interactions between microfilaments and tight junctions in rat hepatocytes during extrahepatic cholestasis induced by common bile duct ligation. *Histochem. Cell Biol* 1996; **106**: 573-580
23 **Wang YJ,** Gregory RB, Barritt GJ. Maintenance of the filamentous actin cytoskeleton is necessary for the activation of store-operated Ca2+ channels, but not other types of plasma-membrane Ca2+ channels, in rat hepatocytes. *Biochem J* 2002; **363**: 117-126
24 **Nishimura Y,** Romer LH, Lemasters JJ. Mitochondrial dysfunction and cytoskeletal disruption during chemical hypoxia to cultured rat hepatic sinusoidal endothelial cells: the pH paradox and cytoprotection by glucose, acidotic pH, and glycine. *Hepatology* 1998; **27**: 1039-1049

25 **Shinohara H,** Tanaka A, Fujimoto T, Hatano E, Satoh S, Fujimoto K, Noda T, Ide C, Yamaoka Y. Disorganization of microtubular network in postischemic liver dysfunction: its functional and morphological changes. *Biochim.Biophys.Acta* 1996; **1317**: 27-35

26 **Aufricht C,** Ardito T, Thulin G, Kashgarian M, Siegel NJ, Van Why SK. Heat-shock protein 25 induction and redistribution during actin reorganization after renal ischemia. *Am J Physiol* 1998; **274**: F215-F222

27 **Dalle-Donne I,** Rossi R, Milzani A, Di Simplicio P, Colombo R. The actin cytoskeleton response to oxidants: from small heat shock protein phosphorylation to changes in the redox state of actin itself. *Free Radic Biol Med* 2001; **31**: 1624-1632

28 **Gomes MD,** Cancherini DV, Moreira MA, Rebouças NA. Ischemic preconditioning of renal tissue: identification of early up-regulated genes. *Nephron Exp Nephrol* 2003; **93**: e107-e116

29 **Panasenko OO,** Kim MV, Marston SB, Gusev NB. Interaction of the small heat shock protein with molecular mass 25 kDa (hsp25) with actin. *Eur J Biochem* 2003; **270**: 892-901

30 **Schwartz N,** Hosford M, Sandoval RM, Wagner MC, Atkinson SJ, Bamburg J, Molitoris BA. Ischemia activates actin depolymerizing factor: role in proximal tubule microvillar actin alterations. *Am J Physiol Renal Physiol* 1999; **276**: F544-F551

31 **Arrigo AP,** Landry J. Expression and function of the low-molecular weight heat shock proteins.1994; 335-373

32 **Benndorf R,** Hayess K, Ryazantsev S, Wieske M, Behlke J, Lutsch G. Phosphorylation and supramolecular organization of murine small heat shock protein HSP25 abolish its actin polymerization-inhibiting activity. *J Biol Chem* 1994; **269**: 20780-20784

33 **Wieske M,** Benndorf R, Behlke J, Dolling R, Grelle G, Bielka H, Lutsch G. Defined sequence segments of the small heat shock proteins HSP25 and alphaB-crystallin inhibit actin polymerization. *Eur J Biochem.* 2001; **268**: 2083-2090

34 **Sakamoto K,** Urushidani T, Nagao T. Translocation of HSP27 to sarcomere induced by ischemic preconditioning in isolated rat hearts. *Biochem Biophys Res Commun* 2000; **269**: 137-142

35 **Freshney NW,** Rawlinson L, Guesdon F, Jones E, Cowley S, Hsuan J, Saklatvala J. Interleukin-1 activates a novel protein kinase cascade that results in the phosphorylation of Hsp27. *Cell* 1994; **78**: 1039-1049

36 **Landry J,** Huot J. Modulation of actin dynamics during stress and physiological stimulation by a signaling pathway involving p38 MAP kinase and heat- shock protein 27. *Biochem Cell Biol* 1995; **73**: 703-707

37 **Murashov AK,** Haq IU, Hill C, Park E, Smith M, Wang X, Wang X, Goldberg DJ, Wolgemuth DJ. Crosstalk between p38, Hsp25 and Akt in spinal motor neurons after sciatic nerve injury. *Brain Res Mol Brain Res* 2001; **93**: 199-208

38 **Nakano A,** Cohen MV, Downey JM. Ischemic preconditioning: from basic mechanisms to clinical applications. *Pharmacol Ther* 2000; **86**: 263-275

39 **Carey DJ,** Rafferty CM, Schramm MM. Association of heparan sulfate proteoglycan and laminin with the cytoskeleton in rat liver. *J Biol Chem* 1987; **262**: 3376-3381

40 **Fox JE,** Reynolds CC, Boyles JK. Studying the platelet cytoskeleton in Triton X-100 lysates. *Methods Enzymol* 1992; **215**: 42-58

41 **Smith PK,** Krohn RI, Hermanson GT, Mallia AK, Gartner FH, Provenzano MD, Fujimoto EK, Goeke NM, Olson BJ, Klenk DC. Measurement of protein using bicinchoninic acid. *Anal Biochem* 1985; **150**: 76-85

42 **Laemmli UK**. Cleavage of structural proteins during the assembly of the head of bacteriophage T4. *Nature* 1970; **227**: 680-685

43 **Kiemer AK**, Baron A, Gerbes AL, Bilzer M, Vollmar AM. The atrial natriuretic peptide as a regulator of Kupffer cell functions. *Shock* 2002; **17**: 365-371

44 **Vesely DL**. Atrial natriuretic peptides in pathophysiological diseases. *Cardiovasc Res* 2001; **51**: 647-658

45 **Sangawa K,** Nakanishi K, Ishino K, Inoue M, Kawada M, Sano S. Atrial natriuretic peptide protects against ischemia-reperfusion injury in the isolated rat heart. *Ann Thorac Surg* 2004; **77**: 233-237

46 **Guay J,** Lambert H, Gingras-Breton G, Lavoie JN, Huot J, Landry J. Regulation of actin filament dynamics by p38 map kinase-mediated phosphorylation of heat shock protein 27. *J Cell Sci* 1997; **110**: 357-368

47 **Cutrin JC,** Cantino D, Biasi F, Chiarpotto E, Salizzoni M, Andorno E, Massano G, Lanfranco G, Rizzetto M, Boveris A, Poli G. Reperfusion damage to the bile canaliculi in transplanted human liver. *Hepatology* 1996; **24**: 1053-1057

48 **McGovern SL,** Shoichet BK. Kinase inhibitors: not just for kinases anymore. *J Med Chem* 2003; **46**: 1478-1483

49 **Kojima K,** Musch MW, Ropeleski MJ, Boone DL, Ma A, Chang EB. Escherichia coli LPS induces heat shock protein 25 in intestinal epithelial cells through MAP kinase activation. *Am J Physiol Gastrointest Liver Physiol* 2003; **286**: G645-G652

50 **Stacchiotti A,** Rezzani R, Angoscini P, Rodella L, Bianchi R. Small heat shock proteins expression in rat kidneys treated with cyclosporine A alone and combined with melatonin. *Histochem J* 2002; **34**: 305-312

51 **Vander Heide RS**. Increased expression of HSP27 protects canine myocytes from simulated ischemia-reperfusion injury. *Am J Physiol Heart Circ Physiol* 2002; **282**: H935-H941

52 **Wilhelm SM,** Simonson MS, Robinson AV, Stowe NT, Schulak JA. Cold ischemia induces endothelin gene upregulation in the preserved kidney. *J Surg Res* 1999; **85**: 101-108

53 **Huot J,** Houle F, Marceau F, Landry J. Oxidative stress-induced actin reorganization mediated by the p38 mitogen-activated protein kinase/heat shock protein 27 pathway in vascular endothelial cells. *Circ Res* 1997; **80**: 383-392

54 **Mounier N,** Arrigo AP. Actin cytoskeleton and small heat shock proteins: how do they interact? *Cell Stress Chaperones* 2002; **7**: 167-176

Science Editor Guo SY **Language Editor** Elsevier HK